

**Doping-dependent thermopower of PbTe from Boltzmann transport calculations**

David J. Singh

*Materials Science and Technology Division, Oak Ridge National Laboratory, Oak Ridge, Tennessee 37831-6114, USA*

(Received 26 April 2010; revised manuscript received 8 May 2010; published 27 May 2010)

The thermopower of PbTe as a function of temperature and doping level is reported based on Boltzmann transport calculations using the first principles relativistic electronic structure as obtained with the Engel-Vosko generalized gradient approximation. The results are discussed in relation to experimental data. For  $p$ -type material there is an enhancement at high-doping levels due to the onset of an increased density of states starting  $\sim 0.2$  eV below the valence band edge. This leads to agreement between the calculated thermopower and recent results on PbTe with heavy Tl doping.

DOI: [10.1103/PhysRevB.81.195217](https://doi.org/10.1103/PhysRevB.81.195217)

PACS number(s): 72.20.Pa

**I. INTRODUCTION**

PbTe is a well-known thermoelectric material.<sup>1-3</sup> It shows good thermoelectric performance for both  $p$ -type and  $n$ -type samples in the important temperature range from ambient to 600 °C. Thermoelectric performance is characterized by a dimensionless figure of merit,  $ZT = \sigma S^2 T / \kappa$ , where  $S$  is the thermopower,  $T$  is temperature,  $\sigma$  is electrical conductivity and  $\kappa$  is the thermal conductivity, which is generally the sum of lattice and electronic contributions,  $\kappa = \kappa_l + \kappa_e$ . The thermopower  $S(T)$  plays a central role in thermoelectric performance, because the  $\kappa_e$ , which forms a lower bound for  $\kappa$ , and  $\sigma$  are connected through the Wiedemann-Franz relation,  $\kappa_e = L\sigma T$ , where  $L$  is the Lorentz number (thus,  $ZT$  will not be more than  $S^2/L$ ).

There is no known upper bound on  $ZT$ , but materials that have  $ZT$  higher than unity are rare.<sup>4</sup> Nonetheless, two new materials based on PbTe with higher  $ZT$  have been reported recently, a nanostructured material, based on PbTe with addition of AgSbTe<sub>2</sub> (denoted LAST) or CdTe,<sup>5,6</sup> and PbTe with Tl as a dopant.<sup>7</sup> In Tl doped PbTe, the origin is thought to be a resonant enhancement of the density of states and therefore  $S$ . In the case of LAST a reduced thermal conductivity, presumably due to the nanostructured nature of the material, has been identified as the origin of the high  $ZT$ . In this regard, PbTe may be particularly interesting as a nanostructured material because it is known to be near lattice instabilities, in particular ferroelectricity, which may be helpful in realizing lower thermal conductivity.<sup>8,9</sup>

There have also been recent papers on possible enhancements of  $S(T)$  in PbTe due to tunneling effects such as energy filtering at grain boundaries and other interfaces.<sup>10-16</sup> However, interpretation of these experiments is complicated by the nontrivial electronic structure of PbTe (see below), sensitivity to the doping level, which may be difficult to control, and extrinsic effects including oxidation in ceramic samples with grain boundaries. Importantly, normal scaling relations for the thermopower are questionable in PbTe because of its nonparabolic band structure. In particular, as discussed below, the shape of the energy bands in PbTe suggests that at high doping and high  $T$  the effective mass entering the thermopower may be higher than that controlling the resistivity, even though only a single band may be active, and that this effect may be  $T$  dependent. We note that there

has been recent progress in achieving controlled high level  $n$ -type doping of PbTe,<sup>17</sup> and also that the resonantly enhanced PbTe:Tl has very high  $p$ -type doping. The purpose of this paper is to provide predictions of the dependence of the thermopower of PbTe on carrier concentration and temperature within Boltzmann theory using the full electronic structure. These provide a baseline for understanding possible enhancements of  $S(T)$  due to non-band-structure effects.

**II. APPROACH**

The calculations were performed using the general potential linearized augmented plane-wave (LAPW) method<sup>18</sup> as implemented in the WIEN2K code.<sup>19</sup> LAPW sphere radii of 2.9 Bohr were used for both Pb and Te. The calculations were done for the experimental rocksalt crystal structure with lattice parameter,  $a = 6.464$  Å. This simple structure greatly facilitates calculations. Well-converged basis sets and zone samplings were used. These were based on  $Rk_{\max} = 9.0$ , where  $R$  is the smallest LAPW sphere radius and  $k_{\max}$  is the interstitial plane-wave cutoff. Additional local orbitals were used for the Pb  $d$  states, which were included as semicore states as well as the Te  $s$  states. The zone sampling, which is important in transport calculations, was done using a  $48 \times 48 \times 48$  reciprocal space mesh. The core states were treated relativistically, while spin-orbit was included for the valence states through the second variational step.

The transport calculations were done using Boltzmann transport theory<sup>20-22</sup> with the constant scattering time approximation. This approximation, which is commonly applied for metals and degenerately doped semiconductors, is based on the assumption that the scattering time determining the electrical conductivity does not vary strongly with energy on the scale of  $kT$ . It does not involve any assumption about the possibly strong doping and temperature dependence of  $\tau$ . The advantage of using this approximation is that the thermopower  $S(T)$  can be calculated without adjustable parameters. This has led to a number of successful applications to thermoelectric materials, including conventional materials and oxides.<sup>22-29</sup> Here, we used the BOLTZTRAP code<sup>30</sup> to perform the needed Brillouin zone integrations.

One difficulty with such calculations is that the band gaps of semiconductors are generally underestimated using standard density functionals. For small band gap thermoelectrics,

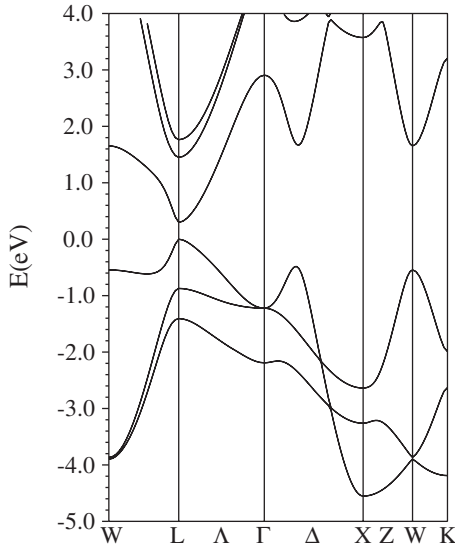


FIG. 1. Calculated band structure of PbTe using the Engel-Vosko GGA.

such as PbTe, the thermopower can be reduced at high temperature and low doping due to bipolar conduction. This effect would be overestimated if the band gap is underestimated. We used the Engel-Vosko generalized gradient approximation (GGA) (Ref. 31) to avoid this. Standard GGA functionals are based on the total energy in terms of the coupling constant averaged exchange correlation hole and are designed to reproduce the total energy.<sup>32</sup> The Engel-Vosko GGA was constructed to reproduce the true exchange correlation potential instead. It yields improved band gaps at the expense of the total energy. The Engel-Vosko GGA is expected to be important especially for high temperatures and low-doping levels, which is the regime where bipolar conduction can reduce the thermopower.

### III. ELECTRONIC STRUCTURE

The calculated band structure is shown in Fig. 1. As may be seen, it is similar to previous density functional calculations except that the band gap is larger.<sup>33</sup> The band gap with the Engel-Vosko GGA is  $E_g=0.299$  eV. This agrees well with the experimental band gap at room temperature and above, which varies between 0.28 eV and 0.36 eV.<sup>6,34–36</sup> It is important to note that both the valence and conduction bands are highly nonparabolic, with the implication that transport should not be modeled using the simple parabolic band expressions. This was discussed in detail early on, although the band structure models used were quite different from the calculated bands.<sup>10,37</sup> An important feature of the band structure is that it becomes much heavier as the Fermi energy is lowered a few tenths of an eV into the valence bands. This is particularly noticeable along the  $L$ – $W$  line where there is an anticrossing a rather flat upward dispersion of the highest band approaching  $L$ . However, as discussed below, the bands become heavier much closer to the band edge, starting at  $\sim 0.2$  eV.

This nontrivial band structure is also relevant to the band gap. Electrical measurements indicate a band gap of

$\sim 0.3$  eV,<sup>38</sup> while optical experiments indicate a band gap with a strong nearly linear  $T$  dependence below 400 K, and constant above.<sup>36</sup> This is an unusual and difficult to understand form. An important issue is the fact that PbTe tends to form with substantial defect concentrations and it is very difficult to obtain undoped, intrinsic PbTe.<sup>10,38</sup> One possibility is that the smaller, low-temperature value of the band gap of  $\sim 0.2$  eV quoted from  $T$ -dependent optical experiments is an artifact of the fits of the optical spectra in a material with doping, Urbach tails, and a highly nonparabolic band structure. Here we assume that the observed  $T$  dependencies come from Fermi broadening and a conventional weakly  $T$  dependent but highly nonparabolic band structure rather than a strongly  $T$  dependent band structure. Based on this we calculate the thermopower with the electronic structure obtained with the Engel-Vosko GGA. The key features of the band structure that are important for the discussion below are the Kane-like shape near the band edge, which means a light mass and a region of nearly linear dispersion, followed at higher energy away from the band edge by an outward curvature of the bands that leads to a much enhanced density of states for both  $p$ -type and  $n$ -type dopings, though this happens closer to the band edge for  $p$  type. It should be noted that besides the band gap, the Engel-Vosko GGA predicts a band structure very similar to other density functionals, such as the local density approximation.

### IV. THERMOPOWER

The doping dependence of the thermopower is shown for various temperatures in Fig. 2, while the  $T$  dependence is shown in Fig. 3. The doping dependence of the thermopower at 300 K in comparison with experimental data is given in Fig. 4. The  $T$ -dependent thermopowers show high values up to the highest doping levels, with a shift in the maximum to higher  $T$  as the doping level is increased for both  $p$ -type and  $n$ -type materials. This is consistent with the known thermoelectric behavior of PbTe.

Harman and co-workers<sup>39</sup> published an extensive set of doping dependent thermopowers for  $n$ -type PbTe based on high-quality Bridgeman grown samples. These include doped with various impurities, including Bi and Cl. The data shows a high level of consistency. The thermopowers at 300 K are very well fit by a Pisarenko form,  $S(n)=a+b \log_{10}(n)$ , with  $a=-477$   $\mu\text{V}/\text{K}$  and  $b=+175$   $\mu\text{V}/\text{K}$  when  $n$  is in units of  $10^{17}$   $\text{cm}^{-3}$ . The deviations from this fit are at the level of  $\sim 10$ – $20$   $\mu\text{V}/\text{K}$ . The main deviation is that the points in the doping range  $\sim 5 \times 10^{17}$ – $5 \times 10^{18}$   $\text{cm}^{-3}$  fall systematically at lower magnitudes of the thermopower than the fit line. The lower panel of Fig. 4 shows the level of agreement between this fit and our calculated thermopower. As may be seen, the agreement is excellent, except at very high-doping levels above  $2 \times 10^{19}$   $\text{cm}^{-3}$  where our calculated values are higher in magnitude than the fit line. This type of deviation from the Pisarenko form at high carrier concentration is to be expected, since the thermopower should not cross zero at the doping level implied by the fit (note that the crossing point amounts to an electron concentration of only  $\sim 0.3\%$ , i.e., an  $n$ -type doped material

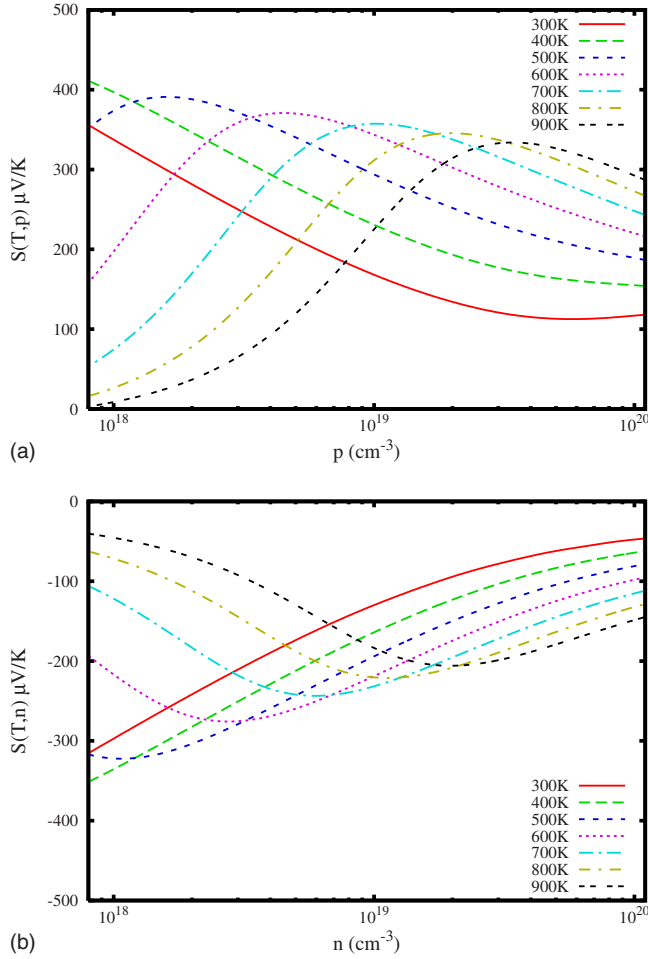


FIG. 2. (Color online) Calculated doping dependence of the thermopower for  $p$ -type (top) and  $n$ -type (bottom) PbTe at various temperatures.

and not a near half filled band metal). It should, however, be mentioned that the last data points in Ref. 39, which are at  $n=2.1 \times 10^{19} \text{ cm}^{-3}$  ( $S=-77 \text{ } \mu\text{V/K}$ ),  $n=2.8 \times 10^{19} \text{ cm}^{-3}$  ( $S=-54 \text{ } \mu\text{V/K}$ ),  $n=3.8 \times 10^{19} \text{ cm}^{-3}$  ( $S=-26 \text{ } \mu\text{V/K}$ ), and  $n=3.9 \times 10^{19} \text{ cm}^{-3}$  ( $S=-25 \text{ } \mu\text{V/K}$ ), do apparently follow the Pisarenko form. One possible explanation is that very heavy doping sometimes leads to nonuniform samples, and this may have happened. In any case, we find the same deviation toward smaller magnitude of  $S$  than the fit line in the range  $\sim 5 \times 10^{17} - 5 \times 10^{18} \text{ cm}^{-3}$  as in the data, so that at least up to  $n=10^{19} \text{ cm}^{-3}$  there is excellent agreement between the calculated and experimental thermopowers.

The situation for  $p$ -type is more complicated, partly because of the lack of a large consistent set of experimental data to compare with. It is common to compare data of  $p$ -type PbTe with a fit by Crocker and Rogers.<sup>40,41</sup> This fit is based on a model and deviates quite substantially from the measured data, and in particular falls well below the measured data in the range  $\sim 10^{18} - 10^{19} \text{ cm}^{-3}$ . Therefore, we do not show the fit, but instead show the raw data from Ref. 40 along with our calculated curve. In addition we show experimental data from Ref. 11, which is for a sintered ceramic formed from a nanopowder with grain sizes from 100 nm to

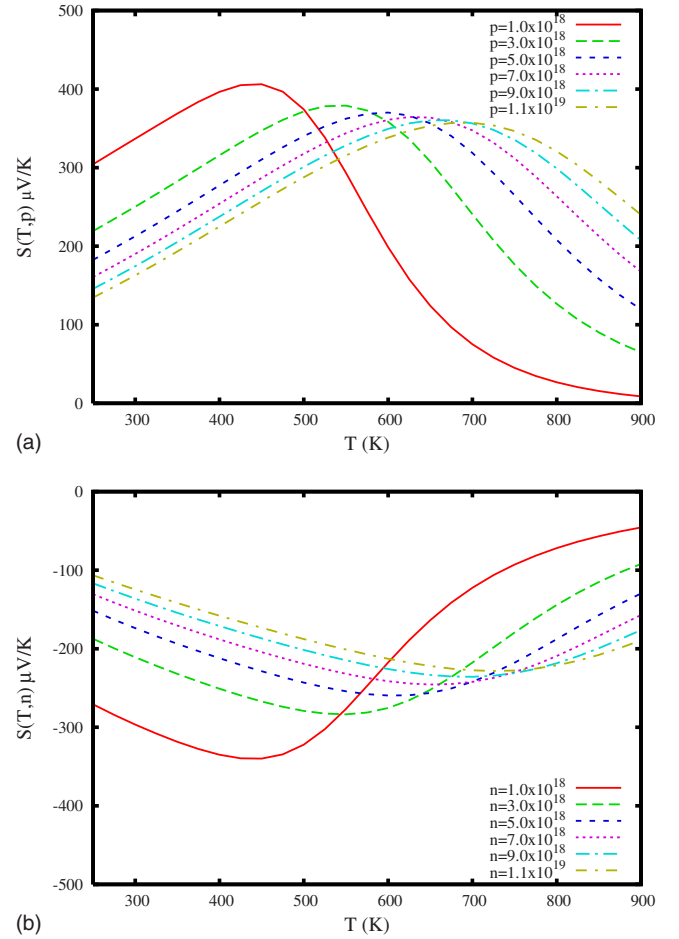


FIG. 3. (Color online) Temperature dependence of the thermopower for various  $p$ -type (top) and  $n$ -type (bottom) doping levels.

$> 1 \text{ } \mu\text{m}$ , as well as the resonantly enhanced PbTe:Tl from Ref. 7. As may be seen, the calculated results agree very well with the data in the low to moderate doping regime but lies well above the data of Crocker and Rogers for high doping levels starting at  $p=10^{19} \text{ cm}^{-3}$ . The data of Martin and co-workers<sup>11</sup> agree well with the calculated curve and are consistent with the data of Ref. 40, although there is an enhancement with respect to the Crocker-Rogers fit.

The PbTe:Tl thermopower data of Heremans and co-workers,<sup>7</sup> which are in the range  $p \sim 4 \times 10^{19} \text{ cm}^{-3}$ , are clearly substantially higher than the data of Crocker and Rogers, but are in reasonable accord with our calculated line, which is also strongly enhanced at high doping levels. This is a consequence of the increasing effective mass below the valence band edge, as mentioned above. It is also interesting to note that both the data and the calculations show only weak doping level dependence of the thermopower in this range of carrier concentrations. One possibility suggested by this result is that the behavior observed is at least in part due to the band structure of PbTe. This explanation would require the assumption that the high-doping level data of Ref. 40 has a low-measured thermopower for extrinsic reasons such as nonuniform doping related to the solubility limit of the dopants for example and that the data of Heremans and co-workers represent intrinsic behavior of very heavily doped

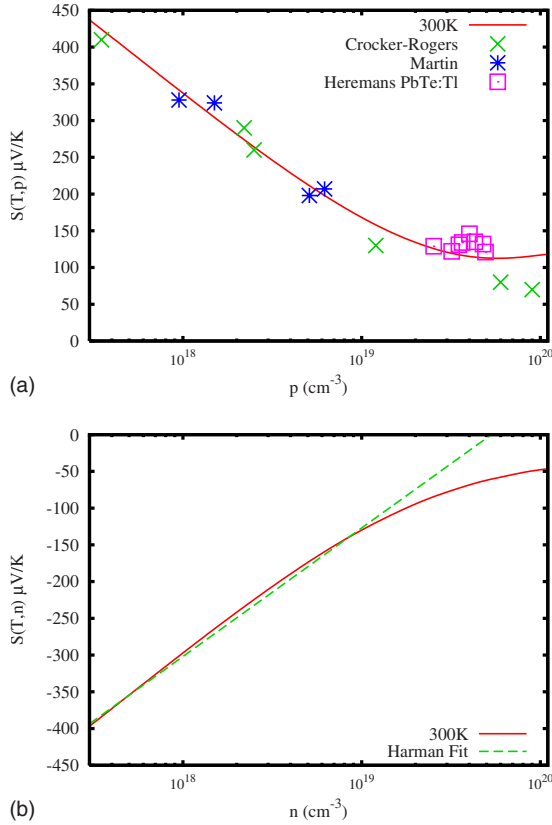


FIG. 4. (Color online) Comparison of the 300 K thermopower of PbTe as a function of doping with experimental data (see text) for *p*-type (top) and *n*-type material (bottom).

PbTe. In order to examine this possibility further, we plot in Fig. 5 the calculated *T* dependence of the thermopower for very heavily doped PbTe in the range measured for PbTe:TI. The doping dependence is weak, as seen experimentally. More importantly these curves are in very good quantitative agreement with the data of Heremans and co-workers, including features such as the upward curvature near ambient *T* and the start of saturation at  $\sim 700$  K and  $300 \mu\text{V/K}$  depending on the exact carrier concentration. Importantly, our calculated results, and the data of Ref. 7 interpreted in this way both imply an enhancement of the thermopower of PbTe

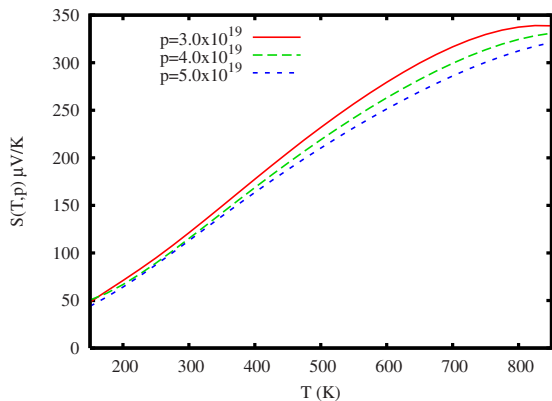


FIG. 5. (Color online) Temperature dependence of the thermopower of PbTe for heavy *p*-type doping.

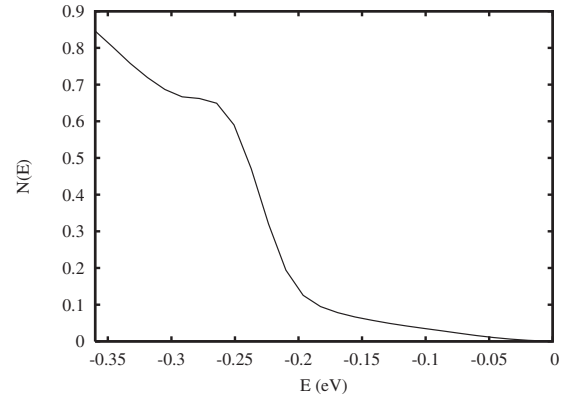


FIG. 6. Electronic density of states for PbTe showing the upper part of the valence bands. The band edge is at 0 eV. A broadening of 0.0136 eV (1 mRy) has been applied.

at elevated *T* and doping level. This can be understood in terms of band structure as follows.

Within Boltzmann theory the transport parameters in a degenerately doped semiconductor at low *T* are written as integrals over the Fermi surface of band structure quantities and scattering rates, while at finite *T*, the formulas are the same, but involve integrals with Fermi distributions. At low *T* the thermopower is given by the Mott formula,  $S_{xx}(T) = (\pi^2 K^2 T / 3e) [d \ln(\sigma_{xx}) / dE] |_{E=E_F}$  for the *x* direction and similarly for the other components. In the constant scattering time approximation  $\sigma_{xx}$  is proportional to the integral of the squared band velocity,  $v_x^2$ , over the Fermi surface multiplied by the inverse scattering rate,  $\tau$ . The finite *T* formulas are similar, but involve Fermi broadening so energy derivative is taken by integrating with  $Ef'(E)$ , where  $f'$  is the derivative of the Fermi function, amounting to a broadened version of the derivative operator. Because of this functional form the conductivity is dominated by the band structure within  $\sim 3kT$  of the chemical potential, while the energy factor in the formula for *S*(*T*) brings in contributions from higher energy, within  $\sim 5kT$ . Therefore the presence of a heavier effective mass away from the band edge may be expected to more strongly affect the thermopower than the conductivity. This may be useful in finding new thermoelectric materials because it may provide a general route for obtaining high thermopower and high mobility in the same sample, i.e., a material could have light bands near the chemical potential providing high mobility, while heavier bands further away could enhance the thermopower but not the depress the mobility.

The electronic density of states (DOS) for our calculated band structure is shown for the top part of the valence bands in Fig. 6. As may be seen, the DOS is low at the top of the valence bands reflecting the light mass nonparabolic Kane-like shape of the valence band edge. However, there is an onset of much heavier behavior starting at  $\sim 0.2$  eV below the edge, and there is a structure that is reminiscent of the shape of a resonance near 0.25 eV. This strongly increasing density of states below 0.2 eV is the reason for the unusual doping and *T* dependent thermopower. This density of states arises because the bands are flat along lines joining the different *L* points (these are at the centers of the hexagonal

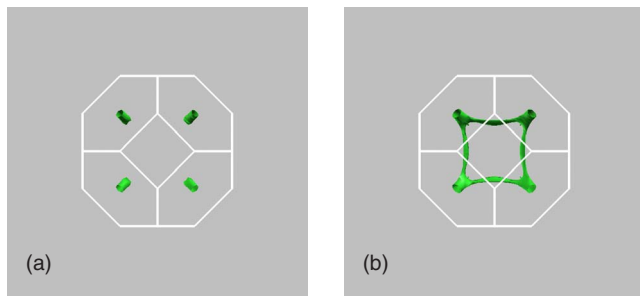


FIG. 7. (Color online) Calculated constant energy surfaces for PbTe 0.2 eV (left) and 0.25 eV (right) below the valence band edge.

faces of the Brillouin zone). This leads to a topology change in the Fermi surface where the  $L$  centered pockets become connected along lines (these are not symmetry lines and the actual connection is only approximately linear) joining them at the position of the DOS peak near 0.2 eV below the band edge. This is illustrated in Fig. 7, which shows constant energy cuts of band structure at binding energies of 0.2 eV and 0.25 eV relative to the band edge. It will be of interest to examine PbTe using techniques such as photoemission, especially angle resolved, to determine if the band structure shows this feature. In any case, this feature leads to an enhancement of the density of states. The onset of this enhancement in the density of states leads to an increased energy dependence of the conductivity and therefore the enhanced thermopower.

It should be emphasized that these calculations have no adjustable parameters and so the  $S(T)$  obtained is strictly a result that arises from the first principles electronic structure.

This is important because data for PbTe has often been analyzed using fits based on a temperature dependent two band models. These have a substantial number of adjustable parameters and do not correspond to the calculated band structure, although they do catch the feature of an onset of heavier mass with hole doping and temperature.<sup>10,36,37,42</sup>

## V. SUMMARY AND CONCLUSION

In summary, we report calculations of the temperature and doping level dependent thermopower in PbTe based on the first principles band structure with no adjustable parameters and no temperature dependence of the electronic structure. We obtain quantitative agreement with experimental data except at very high-doping levels, where the calculated results are higher than the Pisarenko line. Interestingly, for heavily doped  $p$ -type PbTe we obtain agreement with experimental results for resonantly enhanced PbTe:Tl, even though we have no resonant enhancement in the calculations. It will be of interest to study PbTe in more detail, particularly spectroscopically to determine whether this agreement is coincidental or represents intrinsic behavior of PbTe.

## ACKNOWLEDGMENTS

This research was sponsored by the U.S. Department of Energy, Assistant Secretary for Energy Efficiency and Renewable Energy, Office of Vehicle Technologies, as part of the Propulsion Materials Program (transport calculations) and the S3TEC Energy Frontier Research Center (data analysis).

- <sup>1</sup>A. F. Ioffe, *Semiconductor Thermoelements and Thermoelectric Cooling* (Inforsearch, London, 1957).
- <sup>2</sup>C. Wood, *Rep. Prog. Phys.* **51**, 459 (1988).
- <sup>3</sup>D. M. Rowe, *CRC Handbook of Thermoelectrics* (CRC Press, Boca Raton, 1995).
- <sup>4</sup>G. J. Snyder and E. S. Toberer, *Nature Mater.* **7**, 105 (2008).
- <sup>5</sup>K. F. Hsu, S. Loo, F. Guo, W. Chen, J. S. Dyck, C. Uher, T. Hogan, E. K. Polychroniadis, and M. G. Kanatzidis, *Science* **303**, 818 (2004).
- <sup>6</sup>K. Ahn, M. K. Han, J. He, J. Androulakis, S. Balikaya, C. Uher, V. K. Dravid, and M. G. Kanatzidis, *J. Am. Chem. Soc.* **132**, 5227 (2010).
- <sup>7</sup>J. P. Heremans, V. Joavovic, E. S. Toberer, A. Saramat, K. Kurosaki, A. Charoenphakdee, S. Yamanaka, and G. J. Snyder, *Science* **321**, 554 (2008).
- <sup>8</sup>H. Burkhard, G. Bauer, and A. Lopez-Otero, *J. Opt. Soc. Am.* **67**, 943 (1977).
- <sup>9</sup>J. An, A. Subedi, and D. J. Singh, *Solid State Commun.* **148**, 417 (2008).
- <sup>10</sup>Yu. I. Ravich, B. A. Efimova, and V. I. Tamarchenko, *Phys. Status Solidi B* **43**, 453 (1971).
- <sup>11</sup>J. Martin, L. Wang, L. Chen, and G. S. Nolas, *Phys. Rev. B* **79**, 115311 (2009).
- <sup>12</sup>J. Martin, G. S. Nolas, W. Zhang, and L. Chen, *Appl. Phys. Lett.*

- 90**, 222112 (2007).
- <sup>13</sup>K. Kishimoto and T. Koyanagi, *J. Appl. Phys.* **92**, 2544 (2002).
- <sup>14</sup>K. Kishimoto, M. Tsukamoto, and T. Koyanagi, *J. Appl. Phys.* **92**, 5331 (2002).
- <sup>15</sup>J. P. Heremans, C. M. Thrush, and D. T. Morelli, *J. Appl. Phys.* **98**, 063703 (2005).
- <sup>16</sup>R. Madhavaram, J. Sander, Y. X. Gan, and C. K. Masiulaniec, *Mater. Chem. Phys.* **118**, 165 (2009).
- <sup>17</sup>Y. Dong, M. A. McGuire, A. S. Malik, and F. J. DiSalvo, *J. Solid State Chem.* **182**, 2602 (2009).
- <sup>18</sup>D. J. Singh and L. Nordstrom, *Planewaves, Pseudopotentials and the LAPW Method*, 2nd ed. (Springer-Verlag, Berlin, 2006).
- <sup>19</sup>P. Blaha, K. Schwarz, G. Madsen, D. Kvasnicka, and J. Luitz, *WIEN2k, An Augmented Plane Wave+Local Orbitals Program for Calculating Crystal Properties* (K. Schwarz Technical University, Wien, Austria, 2001).
- <sup>20</sup>J. M. Ziman, *Electrons and Phonons* (Oxford University Press, New York, 2001).
- <sup>21</sup>W. Jones and N. H. March, *Theoretical Solid State Physics* (Courier Dover, New York, 1985).
- <sup>22</sup>G. K. H. Madsen, K. Schwarz, P. Blaha, and D. J. Singh, *Phys. Rev. B* **68**, 125212 (2003).
- <sup>23</sup>D. J. Singh and I. I. Mazin, *Phys. Rev. B* **56**, R1650 (1997).
- <sup>24</sup>T. J. Scheidemantel, C. Ambrosch-Draxl, T. Thonhauser, J. V.

- Badding, and J. O. Sofo, *Phys. Rev. B* **68**, 125210 (2003).
- <sup>25</sup>A. F. May, D. J. Singh, and G. J. Snyder, *Phys. Rev. B* **79**, 153101 (2009).
- <sup>26</sup>L. Bertini and C. Gatti, *J. Chem. Phys.* **121**, 8983 (2004).
- <sup>27</sup>L. Lykke, B. B. Iversen, and G. K. H. Madsen, *Phys. Rev. B* **73**, 195121 (2006).
- <sup>28</sup>Y. Wang, X. Chen, T. Cui, Y. Niu, Y. Wang, M. Wang, Y. Ma, and G. Zou, *Phys. Rev. B* **76**, 155127 (2007).
- <sup>29</sup>H. J. Xiang and D. J. Singh, *Phys. Rev. B* **76**, 195111 (2007).
- <sup>30</sup>G. K. H. Madsen and D. J. Singh, *Comput. Phys. Commun.* **175**, 67 (2006).
- <sup>31</sup>E. Engel and S. H. Vosko, *Phys. Rev. B* **47**, 13164 (1993).
- <sup>32</sup>J. P. Perdew, J. A. Chevary, S. H. Vosko, K. A. Jackson, M. R. Pederson, D. J. Singh, and C. Fiolhais, *Phys. Rev. B* **46**, 6671 (1992).
- <sup>33</sup>D. I. Bilc, S. D. Mahanti, and M. G. Kanatzidis, *Phys. Rev. B* **74**, 125202 (2006).
- <sup>34</sup>K. V. Narasimham, J. C. Joshi, K. N. Chopra, C. Jagadish, and A. L. Dawar, *Infrared Phys.* **23**, 349 (1983).
- <sup>35</sup>N. Piccioli, J. M. Besson, and M. Balkanski, *J. Phys. Chem. Solids* **35**, 971 (1974).
- <sup>36</sup>R. N. Tauber, A. A. Machonis, and I. B. Cadoff, *J. Appl. Phys.* **37**, 4855 (1966).
- <sup>37</sup>Yu. I. Ravich, B. A. Efimova, and V. I. Tamarchenko, *Phys. Status Solidi B* **43**, 11 (1971).
- <sup>38</sup>E. Miller, K. Komarek, and I. Cadoff, *J. Appl. Phys.* **32**, 2457 (1961).
- <sup>39</sup>T. C. Harman, D. L. Spears, and M. J. Manfra, *J. Electron. Mater.* **25**, 1121 (1996).
- <sup>40</sup>A. J. Crocker and L. M. Rogers, *Br. J. Appl. Phys.* **18**, 563 (1967).
- <sup>41</sup>L. M. Rogers, *Br. J. Appl. Phys.* **18**, 1227 (1967).
- <sup>42</sup>H. Heinrich, K. Lischka, H. Sitter, and M. Kriechbaum, *Phys. Rev. Lett.* **35**, 1107 (1975).